Chemical Engineering Journal 154 (2009) 76–81

Contents lists available at ScienceDirect

Chemical Engineering Journal

journal homepage: www.elsevier.com/locate/cej

# Deactivation kinetics of platinum-based catalysts in dehydrogenation of higher alkanes

Maryam Saeedizad[a,*], Saeed Sahebdelfar[a], Zahra Mansourpour[b]

[a] Catalyst Research Group, Petrochemical Research and Technology Company, National Petrochemical Company, P.O. Box 14458, Tehran, Iran
[b] Departments of Chemical Engineering, Engineering Faculty, Tehran University, P.O. Box 11465-4563, Tehran, Iran

ARTICLE INFO

*Article history:*
Received 8 December 2008
Received in revised form 23 February 2009
Accepted 10 March 2009

*Keywords:*
Dehydrogenation of paraffins
$Pt/Al_2O_3$ catalyst
Catalyst deactivation
Kinetics

ABSTRACT

The deactivation of promoted $Pt\text{-}Al_2O_3$ catalyst in dehydrogenation of $C_{10}$–$C_{14}$ normal paraffins to the corresponding mono-olefins was studied. Two models based on reversible and irreversible main reaction and *n*th order, concentration-independent deactivation kinetic was used. The kinetic parameters were obtained by utilizing non-linear estimation functions of industrial plant time–temperature trajectory data. The reversible reaction model showed a better fit to the plant data. The results were also checked through integral analysis of experimental data. The results of both approaches were consistent and showed a second-order decay law. The activation energies of the dehydrogenation and catalyst decay were found to be $E_A$ = 90 kJ/mol and $E_d$ = 140 kJ/mol, respectively. The larger activation energy for catalyst deactivation compared to that of main reaction implies that catalyst decay is much more temperature sensitive than main reaction.



## 1. Introduction

Linear alkyl benzenes (LAB) are widely used in the manufacture of alkyl sulfonate which are the basis for production of emulsifiers and biodegradable detergents. Catalytic dehydrogenation of higher *n*-paraffins (e.g. detergent-range $C_{10}$–$C_{14}$) is a key step in this process. The resulted mono-olefins then react with aromatics to produce alkylbenzenes, which are finally sulfonated [1].

The dehydrogenation of paraffins to olefin is an endothermic reversible reaction:

$$C_nH_{2n+2} \Leftrightarrow C_nH_{2n} + H_2 \quad \Delta H^0_{298} \approx 120\,\text{kJ/mol} \tag{1}$$

The reaction is accompanied by volume expansion and is limited by chemical equilibrium. Long-chained paraffins are highly prone to cracking and other side reactions. Therefore, to achieve reasonable olefin yields, a catalyst should be used. A typical catalyst is platinum supported on alumina, promoted with an alkali to naturalize the acidic sites of the support and reduce isomerization, cracking, oligomerization and polymerization reactions. The rate of consecutive dehydrogenation of mono-olefins and diolefins is decreased by tin modifier without lowering the rate of paraffin dehydrogenation significantly. The modifier also improves the stability against fouling by heavy carbonaceous materials [2].

In commercial $C_{10}$–$C_{14}$ *n*-paraffins dehydrogenation reaction is carried out in a radial-flow, fixed-bed reactor in the presence of hydrogen at relatively low pressures (200–300 kPa) and moderately high temperatures (400–500 °C). The selectivity to monoalkenes exceeds 90% and typical conversion of *n*-parrafins is 13% [3]. The activity of catalyst drops slowly with time-on-stream. To maintain a constant conversion with the decaying catalyst, the reaction rate is increased steadily by increasing the feed temperature to the reactor. In this way, the useful catalyst life can be extended to more than a month.

The deactivation rate parameters can be obtained through applying experimental or occasionally commercial plant data to kinetic models. Krishnaswamy and Kittrell [4] analyzed the temperature–time data of deactivating catalysts for constant conversion and developed a simple mathematical model based on a single irreversible primary reaction and *n*th order, concentration-independent deactivation. The applicability of the model to hydrocracking and reforming pilot plant data was demonstrated. Some practical aspects of interpretation of temperature–time data for constant conversion policy in continuous reactors are given by Pacheco and Petersen [5].

The theoretical analysis of variable space-velocity concept to determine catalyst deactivation parameters are given by Levenspiel [6] and Petersen and Pacheco [7]. Sapre [8] used this approach to maintain constant conversion for a decaying catalyst. The variable space-velocity experimental technique was demonstrated for the methanol to hydrocarbon process on ZSM-5 catalyst. The rate

* Corresponding author. Tel.: +98 21 44580100 3503; fax: +98 21 44580501.
*E-mail address:* m.saeedizad@npc-rt.ir (M. Saeedizad).

1385-8947/$ – see front matter © 2009 Elsevier B.V. All rights reserved.
doi:10.1016/j.cej.2009.03.017

**Nomenclature**

| | |
|---|---|
| $a$ | catalyst activity |
| $C_i$ | concentration of species i, mol/m$^3$ |
| $C_M$ | Mears criterions |
| $C_{WP}$ | Weisz–Prater criterions |
| $E_A$ | activation energy for the main reaction, kJ/mol |
| $E_d$ | activation energy for catalyst decay, kJ/mol |
| $k_A$ | reaction rate constant, m$^3$/(kg h) |
| $k_{-A}$ | backward reaction rate constant, m$^3$/(kg h) |
| $k'$ | frequency factor |
| $k_d$ | rate constant for catalyst decay, h$^{-1}$ |
| $k_{d0}$ | decay constant at temperature $T_0$, h$^{-1}$ |
| $K_{eq}$ | concentration equilibrium constant, mol/m$^3$ |
| $n$ | deactivation order |
| $r'_A$ | rate of disappearance of A per mass of catalyst, mol/(kg h) |
| $R$ | gas constant (m$^3$ Pa/(kmol K)) |
| $T$ | temperature, K |
| $W$ | weight of catalyst in the reactor, kg |
| $X$ | conversion of key component, A |

*Greek letters*

| | |
|---|---|
| $\beta$ | parameter defined by Eq. (18) |
| $\tau'$ | a capacity factor (catalyst weight per volumetric feed flow rate), kg h/m$^3$ |

*Subscripts*

| | |
|---|---|
| 0 | initial conditions |
| A | alkane |
| B | olefin |
| d | deactivation |

data were then used to determine the temperature–time policy for maintaining constant reactor outlet conversion at a fixed space-velocity.

In this work, the deactivation kinetics of Pt-based catalysts in dehydrogenation of higher normal paraffins is studied by two approaches. The kinetic parameters are obtained by analysis of experimental data and compared with parameters obtained by optimization algorithms using commercial plant data. Unlike the previous studies, the main reaction was a reversible one. The effect of reversibility of the main reaction on the interpretation of the results is discussed.

## 2. Experimental

The catalyst performance tests were conducted in a stainless-steel, fixed-bed, isothermal reactor (Fig. 1) at 440 °C and 0.7 barg using industrial feedstock with a molar hydrogen/hydrocarbon ratio of six. The reactor (ID = 19 mm) was loaded with 10 ml of commercial Pt-Sn-alumina catalyst (2 mm diameter) diluted with 20 ml SiC located between SiC and $SiO_2$ beds to achieve plug flow and isothermal operation . The reactor effluent was analyzed by an online gas chromatograph (Varian CV3800). HP/PONA column of 50 m length, 0.2 mm diameter and 0.5 μm fill thickness and FID detector were used for liquid product analysis.

The industrial data were provided by a commercial plant in a fixed-bed reactor (ID: 2270 mm, *L*: 4980 mm) operating at 0.7 barg. The start of run and end of run temperatures were 470 °C and 495 °C, respectively. As the feed was a mixture of $C_{10}$–$C_{14}$ normal paraffins, along with small amounts of other hydrocarbons (Table 1), to simplify the analysis through using a single paraffin conversion, the feed components were lumped as a representative component ($n$-$C_{11}$) for which the thermodynamic properties were obtained from the literature [9]. This should be a reasonable assumption as the thermodynamic properties of normal paraffins change smoothly with the carbon number

## 3. Modeling

### 3.1. Reaction kinetic modeling

The dehydrogenation of alkanes on Pt-based catalysts has been found to show first-order dependence with respect to alkane and negative half- to zeroth-order dependence in hydrogen concentration [10]. Accordingly, to account for the above concentration dependences and reversibility of the reaction, the following rate

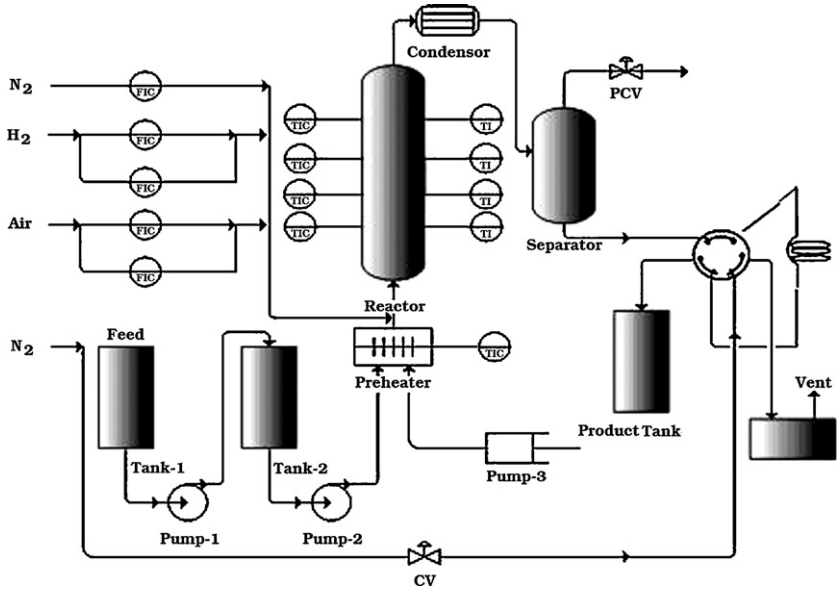


**Fig. 1.** Schematic diagram of the experimental set-up and the reactor.

**Table 1**
Typical paraffin feedstock composition.

| Component | wt% |
|---|---|
| $n$-$C_{10}$ | 7 |
| $n$-$C_{11}$ | 38 |
| $n$-$C_{12}$ | 32 |
| $n$-$C_{13}$ | 21 |
| $n$-$C_{14}$ | 1 |
| Others | 1 |

expression should represent the kinetics:

$$-r'_A = k_A C_A - k_{-A} C_B C_{H_2} = k_A \left( C_A - \frac{C_B C_{H_2}}{K_{eq}} \right) \quad (2)$$

To account for catalyst decay, the catalyst activity, $a$, is incorporated in the rate expression as:

$$-r'_A = k_A a \left( C_A - \frac{C_B C_{H_2}}{K_{eq}} \right) \quad (3)$$

where the activity of the catalyst at time $t$ and temperature $T$, is defined as:

$$a(t, T) = \frac{-r'_A(t)}{-r'_A(t=0)} = \frac{-r'_A}{-r'_{A0}} \quad (4)$$

Because of the high $H_2$/HC molar ratios (~6 mol/mol) commonly employed and the low conversions practiced, the concentration of hydrogen remains constant, in other words, the method of excess is applicable. Similarly, the volume change of reaction can be neglected. Consequently, the reaction rate in terms of paraffin conversion, $X_A$, reduces to:

$$-r'_A = k_A C_{A0} a \left( 1 - \frac{X_A}{X_{Ae}} \right) \quad (5)$$

where $X_{Ae}$ represent equilibrium paraffin conversion. Eq. (5) shows that an increase in temperature results in an increase in the reaction rate both through increasing the rate constant and thermodynamic driving force.

The kinetics of irreversible reactions is simpler to treat because equilibrium conversion calculations are not necessary and, in this case, the results of previous works are mostly applicable to them. Therefore, to check the effect of reversibility, the methodology of estimating kinetic parameters are presented for both cases.

### 3.2. Time–temperature trajectory analysis – irreversible reaction kinetics

For a fixed-bed plug-flow reactor under isothermal conditions:

$$\ln(1 - X_A) = -k_A a \tau' \quad (6)$$

The feed temperature is increased in such a manner that the conversion remains constant with time:

$$X_A(t = 0, T_0) = X_A(t,\ T) \quad (7)$$

To maintain a constant conversion at constant space-velocity:

$$k_{A0} = k_A(T) a(t,\ T) \quad (8)$$

Substituting for $k_A$ in terms of $E_A$, activation energy for the main reaction, from the Arrhenius law, it follows that:

$$k'_{A0} = k'_A e^{(E_A/R)(1/T_0 - 1/T)} a \quad (9)$$

Solving for $1/T$ yields:

$$\frac{1}{T} = \frac{R}{E_A} \ln a + \frac{1}{T_0} \quad (10)$$

The decay law is assumed to be of the following form:

$$-\frac{da}{dt} = k_d a^n \quad (11)$$

where $k_d$ is the deactivation rate constant, exhibiting Arrhenius-type temperature dependence:

$$k_d = k'_d \exp\left( \frac{-E_d}{RT} \right) \quad (12)$$

Substituting Eqs. (10) and (12) into Eq. (11) and rearranging yields:

$$-\frac{da}{dt} = k'_d \exp\left( -\frac{E_d}{E_A} \ln a \right) a^n = k'_d a^{(n - E_d/E_A)} \quad (13)$$

Integrating with $t = 0$, $a = 1$ for $n \neq (1 + E_d/E_A)$:

$$t = \frac{\exp(E_d/RT_0) \left\{ 1 - \exp\left[ \frac{E_d - nE_A + E_A}{R} \times \left( \frac{1}{T} - \frac{1}{T_0} \right) \right] \right\}}{k'_d (1 - n + E_d/E_A)} \quad (14)$$

Eq. (14) shows how the temperature of the reactor should be increased with time in order to maintain the paraffin conversion at a constant level with time [11].

### 3.3. Time–temperature trajectory analysis – reversible reaction kinetics

In the case of a reversible kinetics

$$X_{Ae} \ln\left( 1 - \frac{X_A}{X_{Ae}} \right) = -k_A a \tau' \quad (15)$$

So the following must be satisfied for constant paraffin conversion:

$$\frac{k_A(T) a(t, T)}{X_{Ae}(T) \ln(1 - X_A(T)/X_{Ae}(T))} = \frac{k_{A0}}{X_{Ae}(T_0) \ln(1 - X_A(t = 0, T_0)/X_{Ae}(T_0))} \quad (16)$$

Eq. (16) is more difficult to treat than Eq. (8) because in the former an increase in temperature results in an increase both in the rate constants and thermodynamic driving force for the main reaction (Eq. (5)). Rearranging Eq. (16) gives:

$$k_A(T) a(t, T) = k_{A0} \frac{X_{Ae}(T) \ln(1 - X_A(T)/X_{Ae}(T))}{X_{Ae}(T_0) \ln(1 - X_A(t = 0, T_0)/X_{Ae}(T_0))} = k_{A0} \beta(T) \quad (17)$$

with

$$\beta(T) = \frac{X_{Ae}(T) \ln(1 - X_A(T)/X_{Ae}(T))}{X_{Ae}(T_0) \ln(1 - X_A(t = 0, T_0)/X_{Ae}(T_0))} \quad (18)$$

The parameter $\beta$ accounts for the role of increased thermodynamic driving force on paraffin conversion at higher temperatures. Alternatively upon comparing Eqs. (8) and (17), one observes that $\beta$ is a measure of the suitability of irreversible kinetics assumption. When $X_{Ae}$ approaches to unity $\beta$ becomes unity and Eq. (17) reduces to Eq. (8).

### 3.4. Integral method of analysis – reversible reaction kinetics

For a fixed-bed plug-flow reactor under isothermal conditions in the case of a reversible kinetics:

$$X_{Ae} \ln\left( 1 - \frac{X_A}{X_{Ae}} \right) = -k_A a \tau' \quad (19)$$

**Table 2**
Estimated parameters ($E_A$, $E_d$, $n$, $k_{d0}$).

| | $E_A$ (J/mol) | $E_d$ (J/mol) | $n$ | $k'_d$ ($h^{-1}$) |
|---|---|---|---|---|
| (a) Irreversible reaction | | | | |
| Set1 | | | | |
| N.M. | 99479.2310 | 98925.5113 | 4.1 | 4.39E+03 |
| G.A. | 95091.1296 | 137162.3982 | 4.0 | 1.97E+06 |
| Set2 | | | | |
| N.M. | 91479.0522 | 99456.9066 | 3.5 | 4.29E+03 |
| G.A. | 97782.5808 | 141588.5180 | 4.3 | 3.96E+06 |
| Set3 | | | | |
| N.M. | 96628.4138 | 115730.9783 | 4.7 | 5.81E+04 |
| G.A. | 97763.4537 | 142118.9818 | 4.6 | 3.96E+06 |
| (b) Reversible reaction | | | | |
| Set1 | | | | |
| N.M. | 99431.6382 | 166458.2000 | 1.97 | 1.45E+08 |
| G.A. | 89304.4717 | 152937.6583 | 2.2 | 1.53E+07 |
| | | | | *Set2* |
| N.M. | 109042.2260 | 140907.1650 | 1.96 | 5.93E+06 |
| G.A. | 87292.2192 | 161574.0530 | 2.12 | 7.11E+07 |
| | | | | *Set3* |
| N.M. | 89712.2195 | 111028.1028 | 2.31 | 2.18E+04 |
| G.A. | 73187.6755 | 148437.1100 | 1.88 | 6.34E+06 |

The decay law based on the concentration-independent kinetics and integrating with $t = 0$, $a = 1$ is assumed to be of the following form:

$$a = [1 + (n-1)k_d t]^{1/1-n} \tag{20}$$

Substituting Eq. (20) to Eq. (19) and rearranging yields:

$$F(X_A) = \left[X_{Ae}\ln\left(1 - \frac{X_A}{X_{Ae}}\right)\right]^{1-n} = (-k_A\tau')^{(1-n)} - (n-1)(k_A\tau')^{(1-n)}k_d t \quad n \neq 1 \tag{21}$$

$$F(X_A) = \ln\left(-X_{Ae}\ln\left(1 - \frac{X_A}{X_{Ae}}\right)\right) = \ln k_A\tau' - k_d t \quad n = 1 \tag{22}$$

## 4. Model parameters

The adjustable parameters of the kinetic equations, namely; $E_A$, $E_d$, $n$, $k'_d$ was obtained by minimizing the sum of squares of the residuals (SSR) between plant and experimental data and calculated paraffin conversions using a variety optimization algorithm. Using non-linear optimization functions, experimental data were fitted to Eqs. (14) and (17) then kinetic parameters will be obtained.

### 4.1. Optimization

Two optimization algorithms, Nelder–Mead method and Genetic algorithm were used to estimate the kinetic parameters. The optimizations were performed using Matlab Software (version 7).

## 5. Results and discussion

### 5.1. Application of time–temperature trajectory plant data to models

To obtain kinetic parameters, three sets of time–temperature data obtained from a commercial dehydrogenation plant were employed. These data were taken from a reactor being controlled to maintain constant conversion level of $n$-paraffins. However, because of industrial limitation, an exactly constant conversion was not achieved. These data were then fitted to Eq. (14) and (17) in constant and variable conversion levels, using the aforementioned non-linear parameter estimation functions to estimate the kinetic parameters ($E_A$, $E_d$, $n$, $k_{d0}$).

Table 2 presents the kinetic parameters obtained using these functions. The results for different runs using different optimization algorithms are consistent.

Applying the kinetic parameters into Eq. (14) under constant conversion condition the predicted time–temperature data will be obtained. The goodness of fit, respected by estimated standard errors, defined as follow provided a basis for discrimination between various possible values of $E_a$, $E_d$, $n$, $k_{d0}$.

$$\text{Standard error} = \frac{1}{N}\sum\frac{|y_{Real} - y_{Cal.}|}{y_{Real}} \tag{23}$$

where $N$ is the number of plant data in each set, $y_{Real}$ is the plant data time or temperature and $y_{Cal.}$ is the time or temperature predicted with the model.

As shown in Table 3, the magnitude of mean deviation for each point is very small in G.A. method in irreversible and irreversible reaction, but the small deviations in the other methods confirm that kinetic parameters obtained from all optimization methods are suitable and by applying these parameters into the model one obtains predictions having no significant deviation from experimental data. One observes that the deviation is about one order of magnitude smaller for the cases that the reversibility affects are taken into the account, implying a much better fit of the model with plant data.

Using kinetic parameters obtained by reversible kinetics, average values for order of deactivation, the activation energies

**Table 3**
The amount of mean deviation for each point.

| | Set1 | Set2 | Set3 |
|---|---|---|---|
| (a) Irreversible conditions | | | |
| N.M. | 0.0015 | 0.0022 | 0.0011 |
| G.A. | 0.0011 | 8.7222e−004 | 0.0011 |
| (b) Reversible conditions | | | |
| N.M. | 0.006 | 0.007 | 0.0016 |
| G.A. | 8.3759e−004 | 9.3953e−004 | 6.3268e−004 |

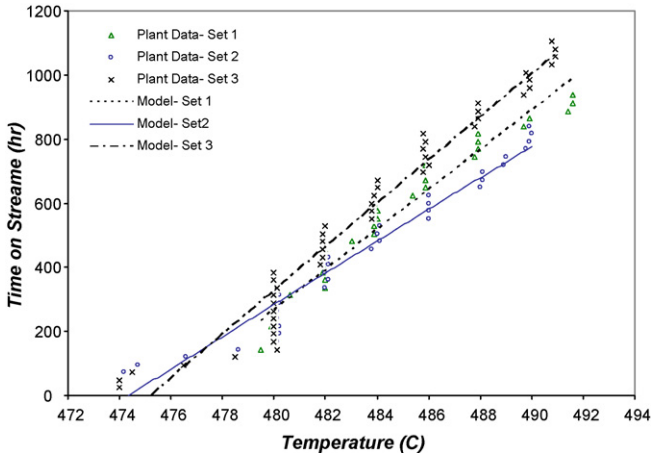


**Fig. 2.** Time–temperature data obtained from parameters estimated with Genetic algorithm method. (Irreversible reaction).

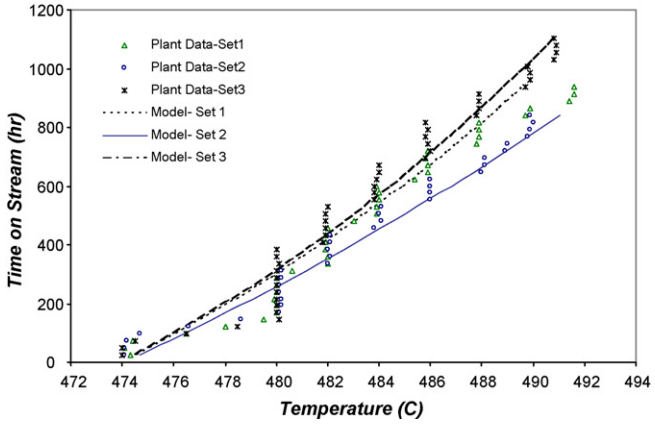


**Fig. 3.** Time–temperature data obtained from parameters estimated with Genetic algorithm method. (Reversible reaction).

of dehydrogenation and catalyst decay are 2.07, 90 kJ/mol and 140 kJ/mol, respectively.

Fig. 2 shows typical time–temperature data obtained from parameters estimated by G.A. function in irreversible condition.

Fig. 3 shows the results obtained from proposed model and temperature–time data for the reversible condition. Most of the experimental data show goodness of fit to the model. Trends of the data represent good agreement with experiment.

As Table 2 illustrates, the activation energy of the catalyst decay is larger than that of the main reaction; therefore the catalyst deactivation is much more temperature sensitive than main reaction.

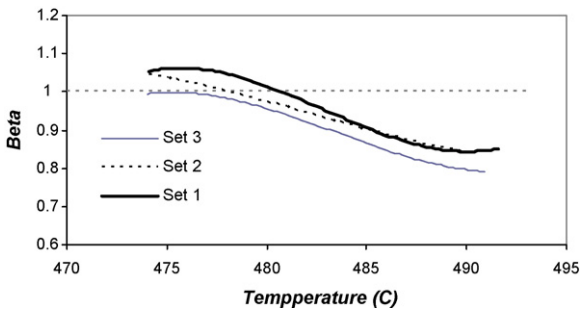


**Fig. 4.** Variation of $\beta$ with the temperature of an industrial reactor.

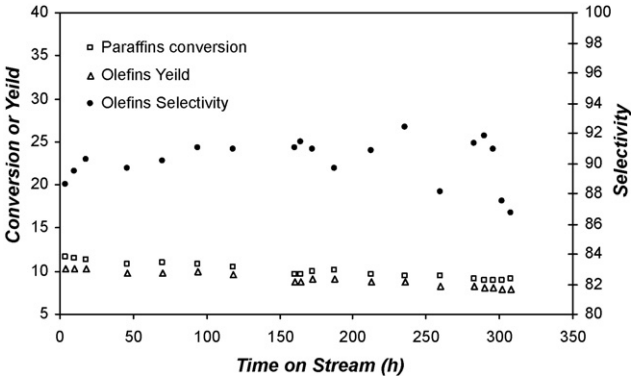


**Fig. 5.** Typical time-on-stream behavior for catalyst dehydrogenation (WHSV = 22.2 $h^{-1}$, $H_2$/HC = 6 mol/mol, $T$ = 440 °C, $P$ = 0.7 barg).

### 5.2. Effects of neglecting reversibility

To test the effect of reversibility, the reversibility term, $\beta$, was calculated. Surprisingly, as Fig. 4 illustrates, $\beta$ is close to unity throughout the temperature range employed. This indicates that within the temperature range of interest, the effect of temperature on the kinetic terms is much more pronounced than that for the thermodynamic driving force (Eq. (18)).

Therefore, neglecting the influence of reversibility in the main reaction rate results in rather small error in the results (see Tables 2 and 3). However, the proposed model based on the reversible main reaction can predict the reactor temperature more precisely.

### 5.3. Integral analysis of experimental data

A long-term time-on-stream performance of catalysts from experimental run is shown in Fig. 5 Activity decreases with a very slow rate as implied by decrease of conversion, because the selectivity remains rather constant (87–92%). A good measure of the overall performance of the catalyst during its life time can be concluded of which the line of olefins yield closely parallels paraffins conversion. The stable selectivity depicted in Fig. 5 is typical of Sn-promoted platinum catalysts and can be explained in geometric term by the dilution of Pt ensembles by Sn. This dilution greatly reduces the activity toward reactions that require a large ensemble of Pt-atoms to constitute active sites, such as hydrogenolysis and coking. Additionally, the carbon deposited during reaction acts the role of inactive species that inhibits undesired reactions [10]. Therefore, although coke deposition adversely affects catalyst activity, it exhibits some beneficial effects on olefin selectivity.

The kinetic expression can be tested against experimental data (time-conversion data) using integral method of analysis [6] with

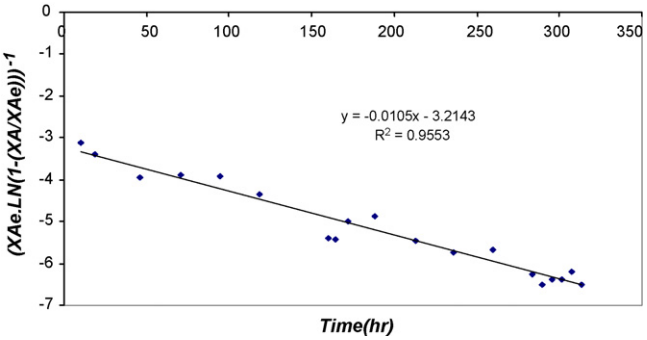


**Fig. 6.** Integral analysis of experimental conversion-time data with $n$ = 2.

various values of order of deactivation ($n$) in Eqs. (21) and (23). Fig. 6 shows a typical plot with $n = 2$, suggesting a second-order decay law. As it is observed, the kinetic models adequately predict the trend in the reduction of conversion and deactivation. This confirms the validity of a second-order decay law for the range of interest. The slope and intercept can be used to estimate the rate constants. From the slope and intercept of Fig. 6, one obtains $k_d = 0.0032\ h^{-1}$ and $k_A\tau' = 0.31$. Considering the operating conditions ($\tau' = 0.0047\ kg\ h/m^3$), the rate constant is found to be $k_A = 66.18\ m^3/kg\ h$.

### 5.4. Mass transfer effects

Mass transfer limitations can influence the apparent kinetic expressions and kinetic parameters as well. Consequently the extent of external and internal mass transfer limitations on $C_{10}$–$C_{14}$ dehydrogenation reaction over Pt-Sn catalyst were also investigated.

Mears and Weisz–Prater criteria show importance of external and internal mass transfer resistance over catalyst. If $C_M \ll 0.15$ and $C_{WP} \ll 1$, external and internal mass transfer resistance will be negligible, respectively [11]. The effective diffusivity and mass transfer coefficient can be estimated from appropriate correlations given elsewhere [12]. In this way, one observes based on maximum reaction rate for Pt-Sn catalyst in $C_{10}$–$C_{14}$ dehydrogenation $C_M = 0.007$ and $C_{WP} = 0.05$, external and internal mass transfer resistance at operating conditions ($P = 1.7$ bar, $T = 480\ ^\circ C$) are negligible and working under the kinetic regime is confirmed.

The Weisz–Prater parameter, however, is not small enough to ensure negligible intra particle diffusion limitation throughout operation. Coking might cause significant diffusion limitation. The presumed series-parallel deactivation implies that uniform cock deposition occurs. On the other hand, significant diffusion limitation (for example, through pore-mouth plugging) could result in a shifting-order decay law which is not confirmed by experimental observations. Consequently, mass transfer limitations should be negligible throughout the useful life of the catalyst in both scales and the reaction rate and kinetic parameters represent the intrinsic ones. This reduce the complexities often arise in scale-up due to the difference in extent of resistances in the two scales.

## 6. Conclusions

A simple mathematical model for catalyst decay in dehydrogenation of linear paraffins was developed. Using industrial plant time–temperature trajectory data, the kinetic parameters were obtained by utilizing non-linear estimation functions. The low error resulted showed that model can predict time–temperature trajectory data under constant paraffin conversion adequately. A nearly second-order decay law was obtained for catalyst deactivation. Since the plant data were used to fit the model, the results are directly applicable to the commercial plant. In particular, the recycled feed used in commercial operation contains higher portions of aromatic constituents and differ widely from chemical grade feeds. Despite their low percentage, aromatics and other impurities in the feed have a significant effect on the catalyst performance.

The deactivation energy is larger than activation energy of the main reaction; therefore the catalyst deactivation is much more temperature sensitive than main reaction.

External and internal mass diffusion effects were investigated through Mears and Weisz–Prater criterions. Results showed that external and internal mass transfer resistances were negligible under operating conditions and the reaction rate and kinetic parameters represent the intrinsic ones.

## Acknowledgments

The authors wish to thank the financial supports form the Research and Technology Company of National Petrochemical Company (NPC-RT). The technical guidance of Dr. Farhad Khorasheh (Sharif University of Technology) and Mr. Mahmoud Beigi (Isfahan Chemical Industries) is also acknowledged with thanks.

## References

[1] Sunggyu Lee, Encyclopedia of Chemical Processing, CRC Press, 2005.
[2] M.M. Bahasin, J.H. McCain, B.V. Vora, T. Imai, P.R. Pujado, Applied Catalysis A: General 1221 (2001) 397.
[3] G.A. Olah, Hydrocarbon Chemistry, Wiley, New York, 2002.
[4] S. Krishnaswamy, J.R. Kittrell, Industrial and Engineering Chemistry Process Design and Development 18 (1979) 399.
[5] M.A. Pacheco, E.E. Petersen, Journal of Catalysis 98 (1986) 380.
[6] O. Levenspiel, The Chemical Reactor Omni Book, Oregon State University Book Store, 1979.
[7] E.E. Petersen, M.A. Pacheco, Fundamental Deactivation Data from Laboratory Reactors, ACS Symposium Series 237 (1984) 365.
[8] A.V. Sapre, Chemical Engineering Science 152 (1997) 4615.
[9] C.Y. Yaws, Chemical Properties Handbook: Physical, Thermodynamic, Environmental, Transport, Safety And Health Related Properties For Organic And Inorganic Chemicals, McGraw Hill Inc, New York, 1999.
[10] I.T. Horváth, Encyclopedia of Catalysis, Wiley, New York, vol. 3. pp 49-79.
[11] H.S. Fogler, Element of Chemical Reaction Engineering, 3rd ed., Printice-Hall, Engelewood Cliffs NJ, 1999.
[12] M. Mohagheghi, G. Bakeri, M. Saeedizad, Chemical Engineering and Technology 12 (2007) 1.